Brain Imaging and Behavior (2010) 4:132–140
DOI 10.1007/s11682-010-9092-1

Regional White Matter Anisotropy and Reading Ability in Patients Treated for Pediatric Embryonal Tumors

Shawna L. Palmer · Wilburn E. Reddick · John O. Glass · Robert Ogg · Zoltan Patay · Dana Wallace · Amar Gajjar

Published online: 9 March 2010

Abstract Children treated with cranial irradiation for brain tumors have reduced white matter volume and deficits in reading ability. This study prospectively examined the relationship between reading and white matter integrity within this patient group. Patients (n=54) were treated with post-surgical radiation followed by 4 cycles of high-dose chemotherapy with stem cell support. At 12 months post-diagnosis, all patients completed a neuropsychology evaluation and a diffusion tensor imaging (DTI) exam. White matter integrity was determined through measures of fractional anisotropy (FA). Significant group differences in FA were found between above average readers and below average readers within the left and right posterior limb of the internal capsule, and right knee of the internal capsule with a trend within the left temporaloccipital region. The integrity of the white matter in these regions may affect communication among visual, auditory, and language cortical areas that are engaged during reading.

Keywords Diffusion tensor imaging · Reading · Pediatric brain tumors · Medulloblastoma

Embryonal tumors arise from the neuroepithelial tissue of the central nervous system (CNS) and include medulloblastomas, primitive neuroectodermal tumors, and atypical teratoid rhabdoid tumors of the brain (Louis et al. 2007). They are the second most common form of brain tumors in children, adolescents and young adults less than 20 years of age (Ries et al. 1999). Due to the inherent risk of CNS dissemination and recurrence, patients diagnosed with embryonal tumors receive aggressive CNS therapy, including maximal surgical resection followed by cranial spinal irradiation and adjuvant chemotherapy. Long-term survivors of such treatments, especially when administered at a young age, are known to be at increased risk for cognitive delays or deficits, impaired academic performance, restricted employment, and diminished quality of life (Oeffinger et al. 2006). Deficits in cognitive abilities following treatment include general intellect, academic achievement, verbal memory, and attention (Briere et al. 2008; Kieffer-Renaux et al. 2000; Mabbott et al. 2008; Mabbott et al. 2005; Nagel et al. 2006; Palmer et al. 2003; Reeves et al. 2006). In 2005 the results of a large prospective study among children with medulloblastoma (n=111) who had received 244 cognitive assessments over a period of 7 years were published (Mulhern et al. 2005). Results showed patients experienced decline in general intellect, spelling and reading decoding ability, with reading showing particular vulnerability. This was especially true for those who were treated at a younger age (<7 years) irrespective of their assessed risk (standard or high).

Diffusion tensor imaging (DTI) is an MRI technique that measures the magnitude and direction of water molecule diffusion within biological tissues (Basser and Jones 2002). This technique is considered to be sensitive to pathological and functional changes within white matter of the brain and thus may be useful in our effort to understand the dynamics of treatment-induced decline of cognitive ability. White matter is an anisotropic tissue with restricted water diffusion due to the myelin sheath, axonal membranes, and close proximity of the fiber bundles. Fractional anisotropy (FA) is a normalized standard deviation of the

This work was presented in part as an abstract at the 13th International Symposium on Pediatric Neuro-Oncology, July 2, 2008, Chicago, IL.

S. L. Palmer (✉) · W. E. Reddick · J. O. Glass · R. Ogg · Z. Patay · D. Wallace · A. Gajjar
St. Jude Children's Research Hospital,
Memphis, TN, USA
e-mail: shawna.palmer@stjude.org

water diffusivities that is calculated from the eigenvalues λ_1, λ_2, λ_3 of the diffusion tensor:

$$FA = \frac{\sqrt{3}}{\sqrt{2}} \frac{\sqrt{(\lambda_1 - \lambda)^2 + (\lambda_2 - \lambda)^2 + (\lambda_3 - \lambda)^2}}{\sqrt{\lambda_1^2 + \lambda_2^2 + \lambda_3^2}}$$

where λ is the mean diffusivity = $(\lambda_1+\lambda_2+\lambda_3)/3$. Diffusion FA increases during the course of myelin development and decreases in areas of damage such as white matter lesions and multiple sclerosis plaques (Barkovitch 2000; Ciccarelli et al. 2001; Klingberg et al. 1999). Among those who are healthy, a relationship between reading skills and a white matter FA of the left temporo-parietal region (Klingberg et al. 2000), left temporal lobe (Nagy et al. 2004) and corona radiata (Qiu et al. 2008) has been found. It is believed that these areas may contribute to reading ability by connecting visual, auditory and language processing regions (Klingberg et al. 2000; Qiu et al. 2008).

Recently, DTI has been used to study white matter in pediatric cancer populations. The first was a small pilot study that included 9 medulloblastoma patients and 9 age matched controls (Khong et al. 2003). The medulloblastoma patients were found to have lower FA in several anatomic sites including cerebellar hemispheres, pons, medulla and periventricular white matter. Additional studies have also demonstrated a reduction in white matter integrity within multiple areas of the brain following treatment, including both the right and left periventricular white matter of the tempo-occipital lobes (Leung et al. 2004), corpus callosum, posterior and anterior limbs of the internal capsule and frontal white matter (Mabbott et al. 2006). Reduction of FA within supratentorial white matter has been associated with deteriorating school performance (Khong et al. 2003). In addition, the percent difference in white matter FA between age-matched patients and controls has been associated with measures of general intellectual ability (Khong et al. 2006; Mabbott et al. 2006). Although these studies employed very small research samples, the use of DTI was established as a valid and sensitive method to detect changes in underlying tissue properties, including damage potentially affecting cognitive outcome.

Although specific cortical regions are purported to underlie reading, the connectivity between regional networks is not straightforward. Following gross total resection, whole brain irradiation, and targeted chemotherapy, the "normal" pathways or networks for reading may be altered. Assuming specific fiber tracts a priori in this population may miss essential pathways that have yet to be identified. Fiber tract analyses are of limited scope and tend to underestimate the spatial extent of changes because they neglect the vast amount of information available in whole head DTI imaging. In addition, these types of studies are also limited by intra-operator variability and reproducibility. In general, voxel-based analysis (VBA) and ROI based analyses give comparable results (Snook et al. 2007).

We report a prospective DTI study to investigate the relationship between reading decoding ability and white matter integrity among a large group of children consistently treated for embryonal tumors. The FA of water diffusion was taken as a measure of the functional integrity of white matter, and a whole brain voxel-based analysis was conducted to identify cluster regions in which white matter FA was associated with measures of reading decoding ability.

Methods

Patient population

Study participants were recruited from an IRB-approved clinical trial for patients newly diagnosed with an embryonal tumor. Written consent was obtained for participation. Patients who were diagnosed with infratentorial medulloblastoma, pineoblastoma, or atypical rhabdoid tumor, at least 1 year from diagnosis, were eligible for the study (n=70). At 12 months post-diagnosis (M=10.2 months, SD=1.08 months) patients must have also completed an MRI examination including DTI imaging sequences and a valid neuropsychological evaluation including an assessment of reading decoding ability. None of the patients had a history of learning disability or traumatic brain injury. Sixteen patients were excluded due to metal artifacts in the MRI examination (n=5), language barriers restricting valid neuropsychology evaluation (n=2), not being physically well enough to be validly assessed (n=4), progressive disease and off study (n=1), parent refusal (n=1), and having completed only a partial evaluation that did not include reading (n=3).

Fifty-four patients (36 males and 18 females) ranging in age from 4.0 to 20.3 years at diagnosis (M=9.8 years, SD=3.8), and from 4.9 to 21.1 years of age at time of evaluation (M=10.67, SD=3.8), were included in the study group. According to enrollment documents 44 patients were White, 6 were Black, 2 were Asian, and 2 were classified as "Other." Using the Edinburgh Inventory (Oldfield 1971) handedness was assessed for 47 of the 54 patients, with 38 being predominantly right handed and 9 predominantly left handed. All patients were treated with post-surgical risk-adapted craniospinal irradiation (CSI) followed by 4 cycles of high-dose chemotherapy (cyclophosphamide, cisplatin, vincristine) with stem cell support: High risk (HR, n=15) patients received CSI to 36–39.6 Gy and conformal boost treatment of the primary site to 55.8–59.4 Gy. The HR patients (n=12 females; n=14 White and 1 Black) were diagnosed with medulloblastoma (n=13) or atypical teratoid rhabdoid tumor (n=2) at an average of 8.7 years of age (SD=3.4). Average-risk (AR, n=39) patients received CSI to 23.4 Gy, conformal

boost treatment to the primary site to 55.8 Gy. The AR patients (n=15 females; n=30 White, 5 Black, 2 Asian, and 2 "Other") were diagnosed with medulloblastoma (n=36), atypical teratoid rhabdoid tumor (n=1) or pineoblastoma (n=2) at an average of 10.23 years of age (SD=3.9).

The general intellectual functioning of the study group was within the average range (M=96.1, SD=18.7). No significant differences between the HR and AR groups were found in intellectual function (M=95.3, SD=24.8; M=97.0, SD=16.4; t=0.28, NS, respectively), age at diagnosis (M=10.2, SD=3.9; M=8.7, SD=3.4; t=0.20, NS, respectively), or age at the time of evaluation (M=11.0, SD=3.9; M=9.6, SD=3.4; t=0.21, NS, respectively).

Reading assessment

Following treatment, all patients completed a protocol driven neuropsychological evaluation at approximately 12 months post-diagnosis using the Woodcock Johnson Tests of Academic Achievement (Woodcock et al. 2001). Two subtests designed to measure reading decoding skill were of particular interest: 1) Word Attack, a reading decoding task using phonologically regular pseudo-words as content. Using phonologically regular pseudo-words as content, rather than common English letters and words, the Word Attack subtest measures reading decoding ability without bias of previous reading experience.

Examinations of reading development have shown children to improve their reading skills as they age (Shaywitz and Shaywitz 2003, 2005). This improvement in reading skill is reflected by the patient successfully completing a greater number of reading subtest items, resulting in a higher raw score. Standard scores are derived from the non-linear transformation of raw scores, allowing performance of a given patient to be compared to the performance of healthy same-age peers. Older children are expected to successfully complete more subtest items (as reflected in higher raw scores) in order to maintain a certain age-adjusted standard score.

Diffusion tensor imaging

Acquisition Diffusion tensor imaging was acquired on one of two 1.5 T Avanto MR imagers (Siemens Medical Systems, Iselin, NJ) using bipolar diffusion-encoding gradients to reduce gradient-induced eddy currents that cause image distortion and degradation (Alexander et al. 1997; Reese et al. 2003). All images were acquired using a double spin echo EPI pulse sequence (TR/TE=10/100 ms, b=1,000 ms). Imaging sets were acquired as forty 3 mm thick contiguous axial sections with whole-head coverage and a 128 square matrix and a 22 cm field-of-view (acquired resolution of 1.7×1.7×3.0 mm). Four acquisitions of thirteen image sets were acquired, one in which b=0 and twelve non-collinear, noncoplanar diffusion gradient directions in which b=1,000 s/mm^2 to calculate the diffusion tensor for each voxel. This acquisition is a compromise to ensure the highest signal to noise possible within a limited amount of time to minimize the risk-benefit ratio for this young vulnerable population.

Analysis Using the 54 image sets, voxel-wise tensor calculations were performed with the DTI toolkit under SPM2 (http://www.fil.ion.ucl.ac.uk/spm/). Data from the four acquisitions were realigned before tensor calculation to correct for linear image drift and the mean of the four realigned image sets were used for tensor calculation. Once the tensors were calculated, Eigen values were derived and used to calculate a fractional anisotropy (FA) map for the whole brain which was then spatially normalized and analyzed in a whole head voxel-based analysis.

Spatial normalization VBA required all examinations be registered into a common stereotactic space. For this project, the original b=0 image from each patient examination was registered to the ICBM average 152T2 atlas aligned in Talairach space found in SPM2, resampled to a 1 mm isotropic resolution. Registration, also referred to as normalization, consisted of a two-step process involving an affine transformation followed by a Free-Form Deformation (FFD) non-linear transformation which corrected for global brain shape differences (Zhang et al. 2008), and were applied to the corresponding FA maps. Both the affine and FFD transformations were part of the VTK CISG Registration Toolkit 2.0 (Rueckert et al. 2003). Default values for the FFD were used in all normalizations.

Voxel-wise statistical testing of the normalized FA images was performed using the VBM Toolkit implemented within SPM2. In preparation for analysis, a binary white matter mask was created by segmenting the T2 atlas using SPM2 and thresholding at a probability of 0.7. The probability threshold selected was empirically determined to include a sufficient proportion of the white matter volume that was common across all subjects. The extent of white matter included in this mask is shown in Fig. 1. Secondly, the normalized FA examinations were all smoothed with a full-width half max 5 mm Gaussian kernel (approximately 125 mm^3 in 3D). According to the Matched Filter Theorem, we could increase the signal-to-noise ratio of our signal when the clusters we were anticipating were on the order of our filter size. Additionally, the choice of a 5 mm FWHM kernel for smoothing is consistent with the generally accepted standard of using a kernel at least 2–3 times the voxel dimension (1.7×1.7×3.0 mm).

Voxel based analysis Since there was only one group and one covariate, a voxel-based analysis was performed to

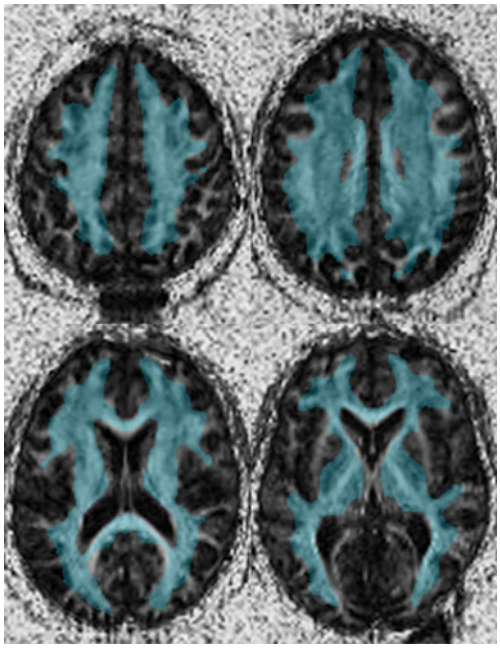

Fig. 1 The binary white matter mask used in the voxel based analysis overlaid on a single patient after spatial normalization. This image demonstrates that while this mask was created from the average FA image from all patients, the majority of the white matter is identified on each individual subject

identify cluster regions within the binary white matter mask with significant associations between FA and reading decoding. The relationship with reading decoding skill was of interest, rather than reading skill as it compares to healthy same-age peers (age-adjusted). Therefore the word attack raw score for each patient was chosen as the covariate for the voxel-based analysis. Utilizing reading decoding raw score also allowed for additional analyses aimed at removing age effects from both FA and reading decoding simultaneously as described below.

No nuisance variables were included and a default 0.1 FA threshold was used in the analysis. Significance ($p<.05$) and cluster threshold (100 voxels) were specified to limit the analysis only to regions that have significant differences and have a sufficient number of continuous voxels for analysis. By using a higher absolute threshold the search area was smaller, positively affecting p-values and correcting for multiple comparisons. A False Discovery Rate approach, which controls the expected proportion of false positives among suprathreshold voxels, was used to account for multiple comparisons (Genovese et al. 2002).

The resulting clusters were overlaid onto the average of the normalized FA images from all subjects for visualization. The voxel coordinates within each significant cluster were extracted using the MARSBAR toolkit within SPM. Average FA values within each cluster, for each patient, were calculated and recorded for subsequent statistical analysis.

Statistical approach

All statistical analyses were conducted using a statistical software package (SPSS for Windows, Version 15.0, 2006. Chicago, IL:SPSS Inc.). The FA values from each identified cluster and raw reading decoding scores were examined in relation to age of the patient at time of examination using bivariate Pearson correlation. Potential differences in FA values and reading decoding between patient risk groups (Average versus High), and handedness groups were explored with one-way analysis of variance (two-tailed).

Both variables utilized in the voxel-based analysis, Word Attack raw scores and observed white matter FA, experience age-related and treatment related change. Therefore regression analyses were completed to remove age-related and treatment-related variance from both variables simultaneously. Age at time of evaluation and

Table 1 Cluster characteristics and the correlation of FA to Word Attack raw score and patient age at evaluation

Cluster	Volume (mm^3)	FA Mean (SD)	Talairach Coordinates Center of Mass			Correlation with FA	
			x	y	z	Word Attack	Age at Eval
L Pons-Medulla Oblongata	399	.425 (.06)	−4.78	−23.8	−45.6	.649***	.699***
R Pons	171	.403 (.07)	8.78	−25.6	−45.2	.684***	.660***
L Posterior Limb of IC	333	.684 (.06)	−12.8	−13.7	−17.2	.531***	.461***
R Posterior Limb of IC	133	.741 (.07)	19.7	−13.2	−7.67	.480***	.315*
L Temporal Occipital	229	.625 (.09)	−37.5	−38.8	−11.9	.567***	.575***
R Knee of IC	527	.634 (.06)	19.4	−2.44	5.57	.633***	.538***
R Occipital Lobe	202	.290 (.07)	12.4	−82.4	15.1	.604***	.488***
L Inferior Parietal	479	.396 (.08)	−19.7	−62.1	23.2	.636***	.558***
Mid-Cingulate	221	.491 (.10)	−5.99	−18.4	21.8	.455**	.577***

L Left; *R* Right; *IC* Internal Capsule

*$p<0.05$, **$p<0.01$, ***$p<0.001$, two-tailed

risk (representing treatment) were placed into the regression model, using the "Enter" method. Separate models were developed for each cluster region to determine if the relationship between FA and reading decoding remained significant after accounting for age and risk.

Results

Significant clusters

Utilizing the voxel based analysis as described above, 9 cluster regions were identified in which FA was associated with word attack raw score; left pons-medulla oblongata, right pons, left and right posterior limb of the internal capsule, left temporal-occipital, right knee of the internal capsule, right occipital, left inferior parietal, and mid-cingulate (Table 1). Review of the T1 imaging from all 54 subjects was completed. These significant clusters were not associated with any T1 changes caused by the tumor.

Reflecting the normal and expected process of white matter maturation, FA values increased as the age of the patient at time of evaluation increased (Table 1). There was no significant difference in FA between Average Risk and High Risk patients within any significant cluster. There was also no significant difference if FA between those predominately left handed versus those who were right handed within any significant cluster.

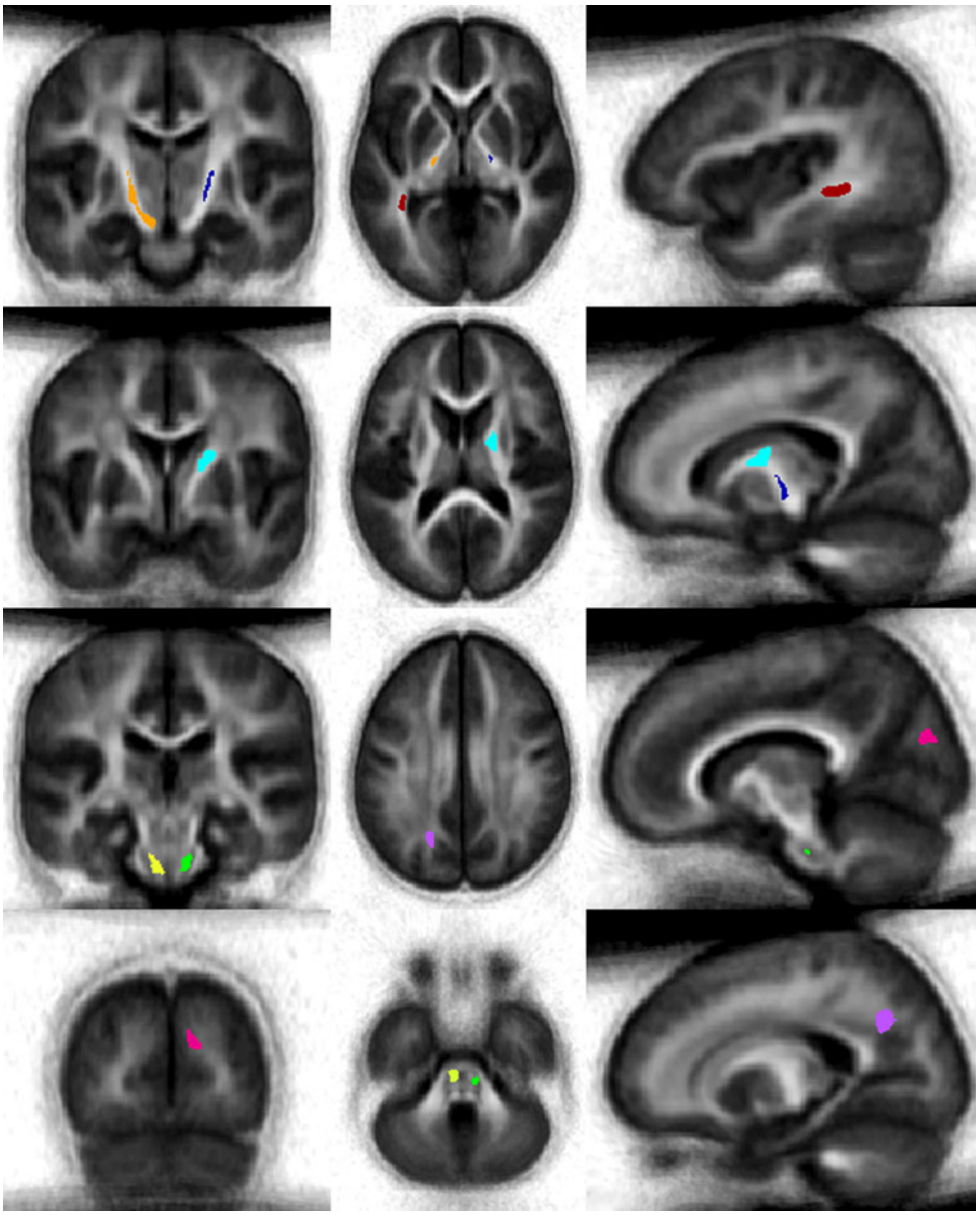

Fig. 2 Average T2 image created from all subjects with eight clusters showing significant associations between reading decoding and FA after controlling for age and treatment: *Orange*—left posterior limb of internal capsule, *Dark blue*—right posterior limb of internal capsule, *Light blue*—right knee of internal capsule, *Dark Red*—left temporal-occipital, *Yellow*—left pons-medulla oblongata, *Green*—right pons, *Magenta*—right occipital, and *Purple*—left inferior parietal

Reading decoding

Examination of reading outcomes and their relationship to age of the patient at time of examination was completed. Indicating reading skill development, Word Attack subtest raw scores improved with increasing age of the patient at time of evaluation ($r(53)=.686$, $p<.001$). There was no significant difference in reading raw scores between Average Risk and High Risk and there was no significant difference in reading raw scores between those predominately left handed versus those who were right handed.

FA and reading decoding

After accounting for age at the time of evaluation and risk, the relationship between FA of each identified cluster and reading decoding ability using Word Attack raw scores as the dependent variable was examined. Results revealed associations between reading decoding and FA within 8 clusters remained significant: left pons-medulla oblongata, right pons, left and right posterior limb of the internal capsule, right knee of the internal capsule, left inferior parietal, right occipital and left temporal occipital cluster (Fig. 2; Table 2).

Discussion

The current study sought to identify cluster regions using tests of reading decoding and measures of white matter FA among a group of children treated for medulloblastoma, pineoblastoma, or atypical rhabdoid tumor. Offering a unique contribution to the literature, nine such clusters were identified, supporting DTI as a useful tool in examining properties of normal-appearing white matter. After controlling for the effects of age of the patient at the time of evaluation and risk, 8 of the clusters were found to remain significantly associated with reading decoding. This result is similar to those described in a recent study of reading development among 75 healthy children including parietal white matter, left and right posterior limb of the internal capsule, and temporal white matter (Qiu et al. 2008).

It is hypothesized that the clusters identified in the current study could represent physical links between cortical areas responsible for word recognition, phonological and semantic skills (Ben-Shachar et al. 2007; Klingberg et al. 2000). Previous literature suggests three neural systems involved in reading ability (Pugh et al. 2001; Shaywitz et al. 2006; Shaywitz and Shaywitz 2003, 2005). The first is referred to as the temporo-parietal reading system and is thought to be important in learning to integrate the written word, or orthography, with corresponding phonological and semantic features; the process of reading decoding. Disruption to the functional integrity of this system has been identified in functional MRI studies among those diagnosed with dyslexia (Shaywitz et al. 2006). The second is referred to as the occipito-temporal system involved in autonomic word recognition, improving speed and fluency in reading. The third system, involved in analysis and articulation, is located in the inferior frontal gyrus or an area long known as Broca's area. This area also serves an important role during silent reading and naming. In a study of non-impaired readers, a strong positive relationship was found between the left hemisphere posterior and anterior reading systems during word analysis (Shaywitz and Shaywitz 2005). In contrast, children considered consistently poor readers also engaged the left posterior reading system but did so differently than their non-impaired peers (Shaywitz et al. 2003). For the poor readers, the left posterior reading system was associated with activation in the right frontal gyri. It is believed that these results may demonstrate compensation on the part of the poor reader. They may rely more heavily on memory-based

Table 2 Multiple regression analyses of average FA within each significant cluster and Word Attack raw score after accounting for age at the time of evaluation and risk

Regression Model*	R^2	F (3, 50) (p-value)	Standardized Coefficient Beta** (p-value)	R^2 Change
L Pons-Medulla Oblongata	.526	18.51 (< 0.001)	.330 (0.020)	.055
R Pons	.566	21.70 (< 0.001)	.410 (0.002)	.095
L Posterior Limb of IC	.531	18.82 (< 0.001)	.276 (0.015)	.060
R Posterior Limb of IC	.555	20.79 (< 0.001)	.310 (0.003)	.084
L Temporal Occipital	.516	17.95 (< 0.001)	.259 (0.036)	.045
R Knee of IC	.576	22.65 (< 0.001)	.390 (0.001)	.105
R Occipital Lobe	.567	21.78 (< 0.001)	.353 (0.002)	.096
L Inferior Parietal	.565	21.66 (< 0.001)	.369 (0.002)	.094

L Left; *R* Right; *IC* Internal Capsule

*Predictors included in model: (constant), age at evaluation, risk, FA of cluster listed

**Beta coefficient and significance of cluster listed after accounting for age at evaluation and risk

rather than methodical word analysis strategies when attempting to decode (Pugh et al. 2001; Shaywitz et al. 2007; Shaywitz and Shaywitz 2005).

A thorough review of reading-related imaging studies utilizing fiber tracking methodology, as well as functional investigations, described four white matter pathways and corresponding cortical areas involved in reading (Ben-Shachar et al. 2007). The first includes occipital temporal callosal fibers connecting posterior occipito-temporal areas that have been found to respond to words and pseudowords in both visual fields. These fibers correspond to the left temporal occipital cluster identified in the current study. The second and third pathways include fibers of the superior lateral fasciculus and a dorsal group that connects to the superior occipital areas. A child who was treated with radiation at age 5, and experiencing profound dyslexia at age 15, underwent several examinations (Rauschecker et al. 2009). Tractography analysis indicated that the patient was missing the left and right arcuate fasciculus within the superior lateral fasciculus. Intersecting with the superior lateral fasciculus are fibers of the fourth pathway, the corona radiata. In addition to fibers from the corona radiata, fibers from the superior lateral fasciculus also pass through the posterior limb of the internal capsule (bilaterally), which could account for the relationship found between FA within this cluster and reading in the current study (Beaulieu et al. 2005; Deutsch et al. 2005).

From our previous studies of reading ability among children treated for embyonal tumors, we know that those who are younger at the time of treatment experience greater deficits in reading decoding ability than those who were

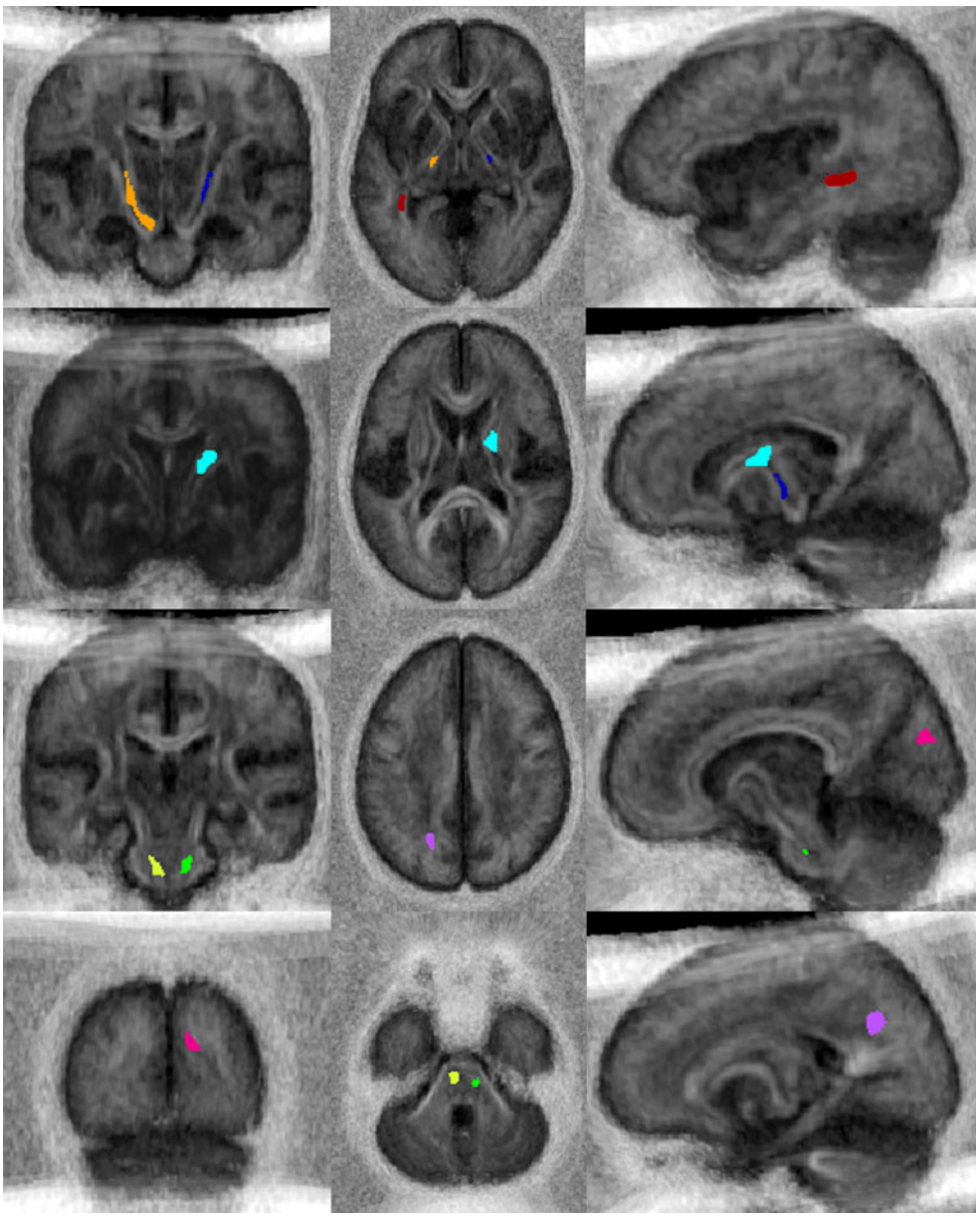

Fig. 3 Standard deviation image computed from the spatially normalized data from all subjects with the eight significant clusters represented: *Orange*—left posterior limb of internal capsule, *Dark blue*—right posterior limb of internal capsule, *Light blue*—right knee of internal capsule, *Dark Red*—left temporal-occipital, *Yellow*—left pons-medulla oblongata, *Green*—right pons, *Magenta*—right occipital, and *Purple*—left inferior parietal. Clusters appear in darker areas with lower standard deviation, thus representing areas with more reproducible spatial normalization

older at the time of treatment (Mulhern et al. 2005). The maturation of the critical white matter pathways may play a key role in the development of reading ability (Beaulieu et al. 2005). Thus, for the younger child with an embryonal tumor, the process of disease and/or treatment may disrupt the normal age-related development of the white matter pathways leading to greater functional deficits in reading decoding ability. However, because the present study applied cross sectional methodology, it is not possible to determine temporal links between the variables of interest. Difficulties in reading skills could be caused by disruption to white matter pathways, as represented by lower measures of FA within the related cluster. However, consistent with ideas of brain plasticity, it could also be that experience with, and the acquisition of, reading decoding skills could impart changes to brain organization (Klingberg et al. 2000; Temple et al. 2003). Future studies could utilize longitudinal methods to examine change within reading-related white matter pathways, reading ability, and their relationship to one another, over time from the point of diagnosis onward. Longitudinal methods would also assist in developing statistical models that would help predict those who are at risk for reading deficits following treatment.

Imaging studies of reading have utilized cohesive groups of right-handed subjects. Handedness is an important consideration to any neuroimaging study aimed at identifying cluster regions associated with cognitive function, especially when examining lateralized functions such as reading skills. Our sample was derived from a clinical treatment protocol where nine patients were predominately left handed. Although FA was not found to significantly differ by handedness, having a small subset of left handed patients may have contributed uncontrolled variance and reduced sensitivity in the statistical analyses.

The current study completed the VBA without consideration of age of the patient, and this could be considered by some as a limitation of the study. Therefore, the VBA was repeated utilizing age of the patient at the time of evaluation as a covariate. The same clusters were identified with the exception of the right posterior limb of the internal capsule. These clusters were usually smaller in the VBA with age but were in the same locations as those originally identified. Shifts in the center of mass of each cluster averaged only 1 mm. Since these clusters lie within the previously identified white matter regions, it was anticipated that FA values would be significantly related. An analysis of the individual subject FA values from each cluster, for both VBA with and without age as a covariate, demonstrated that the FA values were highly correlated (mean r=0.91±.06). These results support the experimental design used in the current study.

This study includes a potential of error associated with the spatial normalization of young undeveloped brains to an adult atlas. The accuracy of the FFD spatial normalization for pediatric cancer patients was established by Zhang et al. (2008) as an average 2 mm error over all pre-defined manual landmarks. The magnitude of this error is well below the full-width half max 5 mm Gaussian kernel used to smooth the examinations. To assess the performance of the spatial normalization, each examination was verified visually for gross distortions or misalignments. While this does not eliminate the possibility of more subtle misalignments of cortical structures, the alignment of deep white matter regions were less likely to be affected. This assessment is consistent with the clarity of the average FA image produced across all subjects. In addition, we produced a standard deviation image reflecting the variance across subjects relative to the average FA image and displayed the eight significant clusters on this image (Fig. 3). Some regions adjacent to the ventricles can be observed to have relatively larger variances across the patient cohort. However, the significant clusters are concentrated within regions of white matter that have the least amount of variance and appear dark on the standard deviation image.

In conclusion, voxel-based analyses identified 9 clusters associated with reading decoding ability of children treated for embryonal tumors. Eight of these clusters remained significant after accounting for age at time of evaluation and risk. These areas may be critical communication pathways between neural reading systems similar to those identified in previous literature. These areas also potentially serve as predetermined regions of interest in longitudinal examinations of white matter integrity and reading decoding, thus assisting in the early detection of those at risk for suffering deficits in reading decoding.

Acknowledgements This work was supported in part by Cancer Center Support (CORE) grant P30CA21765, R01 CA78957, R01CA90246, R01HD49888 and U01CA81445 from the National Cancer Institute and by the American Lebanese Syrian Associated Charities (ALSAC).

References

Alexander, A. L., Tsuruda, J. S., & Parker, D. L. (1997). Elimination of eddy current artifacts in diffusion-weighted echo-planar images: the use of bipolar gradients. *Magnetix Resonance in Medicine, 38*(6), 1016–1021.

Barkovitch, A. J. (2000). Concepts of myelin and myelination in neuroradiology. *American Journal of Neuroradiology, 21*, 1099–1109.

Basser, P. J., & Jones, D. K. (2002). Diffusion-tensor MRI: theory, experimental design and data analysis - a technical review. *NMR in Biomedicine, 15*(7–8), 456–467.

Beaulieu, C., Plewes, C., Paulson, L. A., Roy, D., Snook, L., Concha, L., et al. (2005). Imaging brain connectivity in children with diverse reading ability. *NeuroImage, 25*(4), 1266–1271.

Ben-Shachar, M., Dougherty, R. F., & Wandell, B. A. (2007). White matter pathways in reading. *Current Opinion in Neurobiology, 17*(2), 258–270.

Briere, M., Scott, J. G., McNall-Knapp, R. Y., & Adams, R. L. (2008). Cognitive outcome in pediatric brain tumor survivors: delayed

attention deficit at long term follow-up. *Pediatric Blood Cancer, 50*, 337–340.

Ciccarelli, O., Werring, D. J., Wheeler-Kingshott, C. A., Barker, G. J., Parker, G. J., Thompson, A. J., et al. (2001). Investigation of MS normal-appearing brain using diffusion tensor MRI with clinical correlations. *Neurology, 56*(7), 926–933.

Deutsch, G. K., Dougherty, R. F., Bammer, R., Siok, W. T., Gabrieli, J. D., & Wandell, B. (2005). Children's reading performance is correlated with white matter structure measured by diffusion tensor imaging. *Cortex, 41*(3), 354–363.

Genovese, C. R., Lazar, N. A., & Nichols, T. (2002). Thresholding of statistical maps in functional neuroimaging using the false discovery rate. *NeuroImage, 15*(4), 870–878.

Khong, P. L., Kwong, D. L., Chan, G. C., Sham, J. S., Chan, F. L., & Ooi, G. C. (2003). Diffusion-tensor imaging for the detection and quantification of treatment-induced white matter injury in children with medulloblastoma: a pilot study. *American Journal of Neuroradiology, 24*(4), 734–740.

Khong, P. L., Leung, L. H. T., Fung, A. S. M., Fong, D. Y. T., Qiu, D., Kwong, D. L., et al. (2006). White matter anisotropy in post-treatment childhood cancer survivors: preliminary evidence of association with neurocognitive function. *Journal of Clinical Oncology, 24*(6), 884–890.

Kieffer-Renaux, V., Bulteau, C., Grill, J., Kalifa, C., Viguier, D., & Jambaque, I. (2000). Patterns of neuropsychological deficits in children with medulloblastoma according to craniospatial irradiation doses. *Developmental Medicine and Child Neurology, 42*, 741–745.

Klingberg, T., Vaidya, C. J., Gabrieli, J. D., Moseley, M. E., & Hedehus, M. (1999). Myelination and organization of the frontal white matter in children: a diffusion tensor MRI study. *Neuroreport, 10*(13), 2817–2821.

Klingberg, T., Hedehus, M., Temple, E., Salz, T., Gabrieli, J. D., Moseley, M. E., et al. (2000). Microstructure of temporo-paretal white matter as a basis for reading disability: evidence from diffusion tensor magnetic resonance imaging. *Neuron, 25*, 493–500.

Leung, L. H. T., Ooi, G. C., Kwong, D. L., Chan, G. C. F., Cao, G., & Khong, P. L. (2004). White matter diffusion anisotropy after chemo-irradiation: a statistical parametric mapping study and histogram analysis. *NeuroImage, 21*, 261–268.

Louis, D. N., Ohgaki, H., Wiestler, O. D., Cavenee, W. K., Burger, P. C., Jouvet, A., et al. (2007). The 2007 WHO classification of tumours of the central nervous system. *Acta Neuropathologica, 114*(2), 97–109.

Mabbott, D. J., Spiegler, B. J., Greenberg, M. L., Rutka, J. T., Hyder, D. J., & Bouffet, E. (2005). Serial evaluation of academic and behavioral outcome after treatment with cranial radiation in childhood. *Journal of Clinical Oncology, 23*(10), 2256–2263.

Mabbott, D. J., Noseworthy, M. D., Bouffet, E., Rockel, C., & Laughlin, S. (2006). Diffusion tensor imaging of white matter after cranial radiation in children for medulloblastoma: correlation with IQ. *Neuro Oncology, 8*, 244–252.

Mabbott, D. J., Penkman, L., Witol, A., Strother, D., & Bouffet, E. (2008). Core neurocognitive functions in children treated for posterior fossa tumors. *Neuropsychology, 22*(2), 159–168.

Mulhern, R. K., Palmer, S. L., Merchant, T. E., Wallace, D., Kocak, M., Brouwers, P., et al. (2005). Neurocognitive consequences of risk-adapted therapy for childhood medulloblastoma. *Journal of Clinical Oncology, 23*(24), 5511–5519.

Nagel, B. J., Delis, D. C., Palmer, S. L., Reeves, C., Gajjar, A., & Mulhern, R. K. (2006). Early patterns of verbal memory impairment in children treated for medulloblastoma. *Neuropsychology, 20*(1), 105–112.

Nagy, Z., Westerberg, H., & Klingberg, T. (2004). Maturation of white matter is associated with the development of cognitive functions during childhood. *Journal of Cognitive Neuroscience, 16*(7), 1227–1233.

Oeffinger, K. C., Mertens, A. C., Sklar, C. A., Kawashima, T., Hudson, M. M., Meadows, A. T., et al. (2006). Chronic health conditions in adult survivors of childhood cancer. *New England Journal of Med, 355*(15), 1572–1582.

Oldfield, F. C. (1971). The assessment and analysis of handedness: the Edinburgh Inventory. *Neuropsychologia, 9*, 97–113.

Palmer, S. L., Gajjar, A., Reddick, W. E., Glass, J. O., Kun, L. E., Wu, S., et al. (2003). Predicting intellectual outcome among children treated with 35–40 Gy craniospinal irradiation for medulloblastoma. *Neuropsychology, 17*(4), 548–555.

Pugh, K. R., Mencl, W. E., Jenner, A. R., Katz, L., Frost, S. J., Lee, J. R., et al. (2001). Neurobiological studies of reading and reading disability. *Journal of Communication Disorders, 34*(6), 479–492.

Qiu, D., Tan, L. H., Zhou, K., & Khong, P. L. (2008). Diffusion tensor imaging of normal white matter maturation from late childhood to young adulthood: voxel-wise evaluation of mean diffusivity, fractional anisotropy, radial and axial diffusivities, and correlation with reading development. *NeuroImage, 41*(2), 223–232.

Rauschecker, A. M., Deutsch, G. K., Ben-Shachar, M., Schwartzman, A., Perry, L. M., & Dougherty, R. F. (2009). Reading impairment in a patient with missing arcuate fasciculus. *Neuropsychologia, 47*(1), 180–194.

Reese, T. G., Heid, O., Weisskoff, R. M., & Wedeen, V. J. (2003). Reduction of eddy-current-induced distortion in diffusion MRI using a twice-refocused spin echo. *Magnetic Resonance in Medicine, 49*(1), 177–182.

Reeves, C. B., Palmer, S. L., Reddick, W. E., Merchant, T. E., Buchanan, G. M., Gajjar, A., et al. (2006). Attention and memory functioning among pediatric patients with medulloblastoma. *Journal of Pediatric Psychology, 31*(3), 272–280.

Ries, L., Smith, M., Gurney, J., Linet, M., Tamra, T., Young, J., et al. (Eds.). (1999). *Cancer Incidence and Survival among Children and Adolescents: United States SEER Program 1975–1995* (Vol. NIH Pub. No. 99-4649). Bethesda, MD: National Cancer Institute, SEER Program.

Rueckert, D., Frangi, A. F., & Schnabel, J. A. (2003). Automatic construction of 3-D statistical deformation models of the brain using nonrigid registration. *IEEE Transactions on Medical Imaging, 22*(8), 1014–1025.

Shaywitz, S. E., & Shaywitz, B. A. (2003). Dyslexia (specific reading disability). *Pediatrics in Review, 24*(5), 147–153.

Shaywitz, S. E., & Shaywitz, B. A. (2005). Dyslexia (specific reading disability). *Biological Psychiatry, 57*(11), 1301–1309.

Shaywitz, S. E., Shaywitz, B. A., Fulbright, R. K., Skudlarski, P., Mencl, W. E., Constable, R. T., et al. (2003). Neural systems for compensation and persistence: young adult outcome of childhood reading disability. *Biological Psychiatry, 54*(1), 25–33.

Shaywitz, B. A., Lyon, G. R., & Shaywitz, S. E. (2006). The role of functional magnetic resonance imaging in understanding reading and dyslexia. *Developmental Neuropsychology, 30*(1), 613–632.

Shaywitz, B. A., Skudlarski, P., Holahan, J. M., Marchione, K. E., Constable, R. T., Fulbright, R. K., et al. (2007). Age-related changes in reading systems of dyslexic children. *Annals of Neurology, 61*(4), 363–370.

Snook, L., Plewes, C., Beaulieu, C. (2007). Voxel based versus region of interest analysis in diffusion tensor imaging of neurodevelopment. *Neuroimage, 34*, 243–252.

Temple, E., Deutsch, G. K., Poldrack, R. A., Miller, S. L., Tallal, P., Merzenich, M. M., et al. (2003). Neural deficits in children with dyslexia ameliorated by behavioral remediation: evidence from functional MRI. *Proceedings of the National Academy of Sciences of the Uited States of America, 100*(5), 2860–2865.

Woodcock, R., McGraw, K., & Mather, N. (2001). *Woodcock-Johnson third edition, tests of achievement*. Itasca: Riverside.

Zhang, Y., Zou, P., Mulhern, R. K., Butler, R. W., Laningham, F. H., & Ogg, R. J. (2008). Brain structural abnormalities in survivors of pediatric posterior fossa brain tumors: a voxel-based morphometry study using free-form deformation. *NeuroImage, 42*(1), 218–229.